JOURNAL OF MATERIALS SCIENCE 27 (1992) 3782–3788

Non-linear compression stress–strain curve of pitch-based high modulus carbon fibre composites and structural responses

N. TSUJI, K. KUBOMURA
Chemicals, Advanced Materials and Technology Research Laboratories, Technical Development Bureau, Nippon Steel Corporation, 1618 Ida, Nakahara, Kawasaki 211, Japan

The longitudinal compression behaviour of unidirectional composites is studied to understand the role of the fibre compressive property in deformation and failure by systematically varying the tensile modulus of reinforcing high modulus carbon fibre. As the composites deform, their softness increases with increasing compressive strain, and the loading path is traced back when the load is removed. The intensity of softening is correlated to the fibre's tensile modulus and possible softening mechanisms are discussed in conjunction with fibre and matrix properties. Further, it is investigated how the non-linear stress–strain relation affects the stress and strain distributions and deformation when plates fabricated from these fibres are tested by the three-point bending test.

1. Introduction

To manufacture high modulus carbon fibres, graphite crystallites are made which are highly oriented along the fibre axis and thus the fibres become anisotropic [1]. They behave differently, both in compression and tension, along and transverse to the fibre direction. When these fibres are used as reinforcements in composite materials, their behaviour plays an important role in their deformation and failure. Nevertheless, except for the tensile property along the fibre axis, other fibre properties have not been well characterized because of their extremely small size. Among them, the compressive property plays an especially important role in composite structure integrity. There have been several attempts to measure compressive properties along the fibre axis by methods such as the elastic loop test [2], the bending beam test [3], the compression test of single-fibre composite [4], the recoil test [5] and the critical fibre length method [6]. They either measure the compressive failure strain directly and convert it to the compressive failure stress by multiplying by the tensile Young's modulus, or else they measure the compressive failure stress indirectly. These methods only measure a point in a stress–strain curve such as the strain to failure or the stress to failure, but do not follow a deformation process, i.e. a stress–strain curve. Since in many cases the compressive deformation and failure are associated with buckling in composites, the proper understanding of them requires the fibre stress–strain curve. There is a good chance of predicting the compressive stress–strain relation and failure of fibres by using the longitudinal compression test of unidirectional composites. However, matrix and fibre properties and the behaviour of their interface play their own roles in the composite compressive deformation and failure and these roles are not yet fully understood. Obtaining these properties by a composite test must be done with extreme care.

When plastics are reinforced with highly oriented fibres, they show non-linearities both in tension and compression along the fibre direction. Pitch-based carbon fibre is one of them. However, the unidirectional composite compressive behaviour is at present not accurately predicted by fibre compressive properties, nor is fibre compressive behaviour predicted by the composite compression test. Therefore, the obtaining of longitudinal compressive stress–strain relations of unidirectional composites becomes important for two reasons. First, the composite stress–strain curve and failure mode, which are in many cases different from the tensile ones, may change the structural response, which is predicted by using the material properties deduced from the tensile properties. Secondly, the understanding of fibre compressive deformation and failure mechanisms is needed to get an insight into the fibre's microstructure and to improve the fibre's mechanical properties. In this work, the unidirectional epoxy composite plates reinforced with several high modulus mesophase pitch-based fibres were compression tested and their stress–strain relations were compared with each other as well as with those of unidirectional composites with PAN-based high modulus carbon fibre and aramid fibre. Then we tried to relate fibre microstructures and composite compressive stress–strain curves.

Since non-linear stress–strain relations both in tension and compression alter the location of the beam's neutral axis, formulas for calculating the tensile and compressive stresses of coupons reinforced with these fibres are to be evaluated by using the bending test. Further, when composites with these fibres are used in

0022–2461

TABLE I Tensile properties of fibres and their epoxy composites

	Pitch-based CF					PAN CF	Aramid
	A	B	C	D	G	M40	Kevlar 49
Fibre tensile modulus (GPa)	195	300	400	500	51	400	131
Fibre tensile strength (MPa)	2800	3200	3500	3340	1020	2800	3000
Fibre elongation (%)	1.45	1.07	0.85	0.67	1.98	0.60	2.30
Composite tensile modulus[a] (GPa)	96	137	200	240	26	210	75
Composite tensile strength[a] (MPa)	1350	1500	1760	1670	490	1230	1380

[a] Volume fraction is 60% equivalent.

structures, the advantages and disadvantages associated with non-linearities must be carefully traded off. To illustrate the advantages, the three-point bending test was analysed with the finite-element method considering large deflection and the tensile and compressive non-linear stress–strain relations. In past analyses [7–9] the bending tests of Kevlar 49 unidirectional composites were analysed with the elastic–perfect stress–strain relation. In the present analysis, a relation of softening in compression and hardening in tension is used and the analysis is validated by comparing the test and analysis results, and stress distributions in the coupon are also discussed.

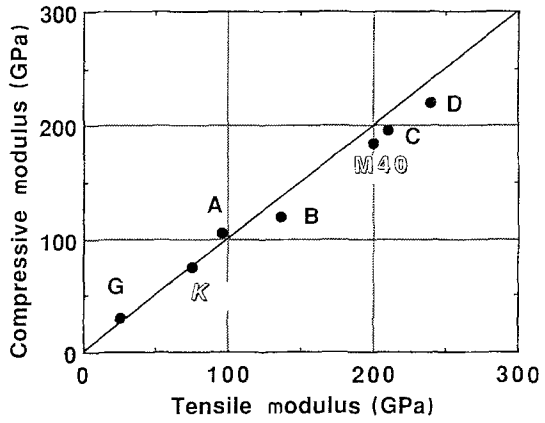

Figure 1 Composite compressive moduli versus tensile moduli.

2. Compression test

Many highly anisotropic fibres, such as high modulus carbon fibres [10] and high performance polymer fibres [3], behave very differently under compressive and tensile loads. The longitudinal tensile properties of these fibre-reinforced unidirectional composites are well understood, while the characterization and the understanding of their compressive failure and deformation mechanisms are not yet fully developed. These properties have been investigated for mesophase pitch-based carbon fibre composites in the present study.

2.1. Test specimen

Unidirectional compression test coupons were fabricated from pitch-based carbon fibres of five different tensile moduli (A, B, C, D, G), aramid fibre (Du Pont Kevlar 49) and PAN-based carbon fibre (Toray Torayca M40). The tensile mechanical properties of the fibres and their epoxy composites are shown in Table I. Pitch-based carbon fibre G was spun from isotropic pitch and fibres A, B, C and D were spun from mesophase pitch. All compression tests were done according to the ASTM procedure A (Celanese Method) [11, 12], in which strains were measured on both sides of the gauge section to detect any bending deformation. When these two strains differed significantly, the test result was discarded.

2.2. Results and discussion

2.2.1. Compressive moduli

In Fig. 1, composite compressive and tensile moduli are shown. For higher tensile modulus fibres B, C, D and M40, the tensile moduli are about 10% larger than the compressive moduli. Although compressive and tensile moduli are supposed to coincide at zero strain, they do not because they are calculated, not from exactly zero strain, but from 0.0 and about 0.005 strains for both compression and tension, and they behave differently even under very small strains.

2.2.2. Compressive strengths

In Fig. 2, composite tensile moduli and compressive strengths are shown, where the composites with fibres, A, B, C and D show strength decreasing almost linearly with increasing modulus. In Fig. 3, composite tensile and compressive strengths are shown. Except for fibre G, which was spun from isotropic pitch, compressive strengths are significantly smaller than tensile strengths.

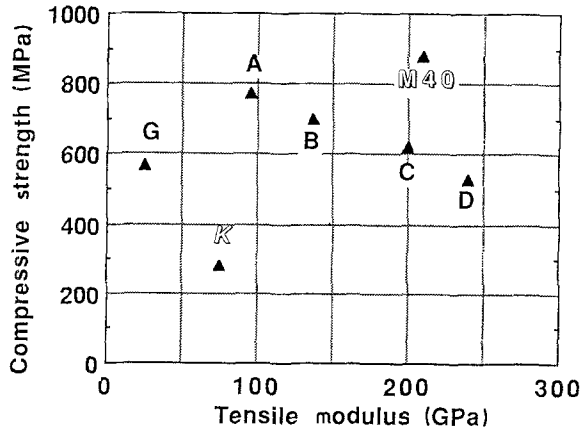

Figure 2 Composite compressive strengths versus tensile moduli.

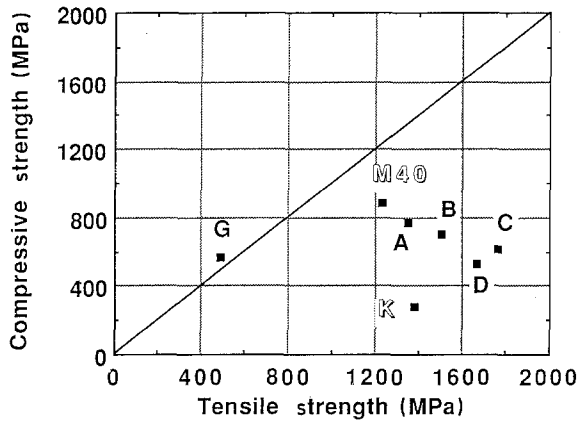

Figure 3 Composite compressive strengths versus tensile strengths.

2.2.3. Load–strain curves

In Fig. 4, load–strain curves in the longitudinal compression test of a unidirectional composite of fibre D are shown, and in Fig. 5 the corresponding Poisson's ratios are shown. As the compressive strain increases, the modulus decreases significantly, up to almost zero, while the Poisson's ratio remains almost constant. At 0.5% strain, which corresponds to about 90% of the compressive failure stress, the tangent modulus is about 30% of the modulus at zero strain. In Fig. 6, load–strain curves are shown for compressive loadings and unloadings of the composite. In this test result, the loading and unloading paths coincide and leave no permanent deformation. This material shows a remarkable reduction in compressive modulus for a small recoverable strain, such as 0.5% strain, while for many materials non-linear stress–strain relations are associated with permanent deformations or large strains.

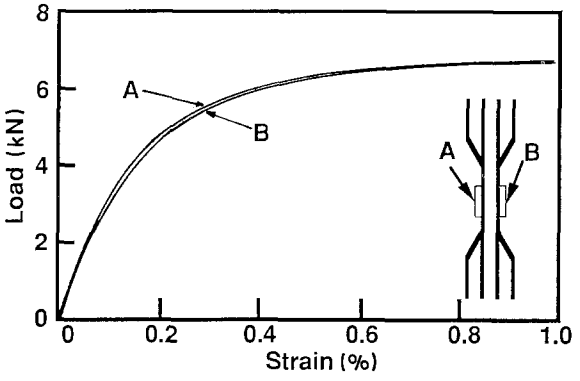

Figure 4 Compressive load–strain curves (fibre D).

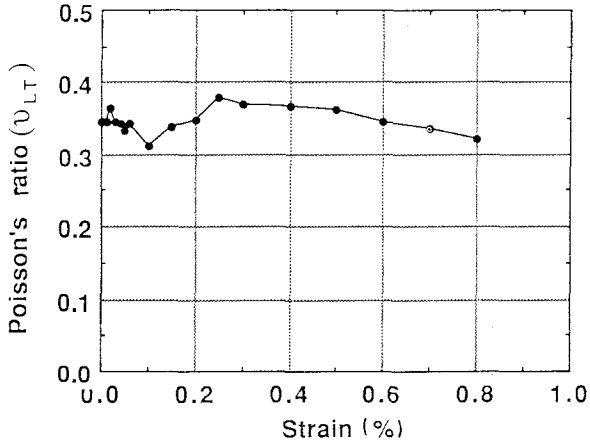

Figure 5 Poisson's ratio versus strain (fibre D).

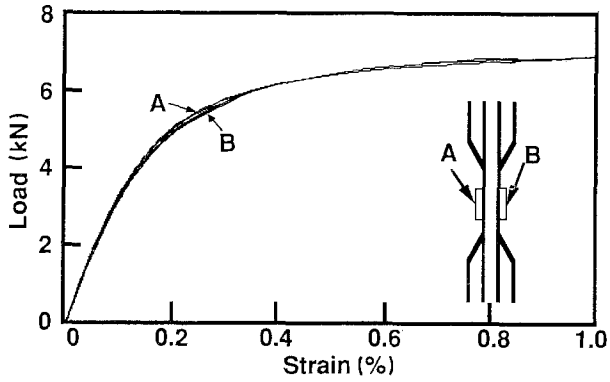

Figure 6 Compressive load–strain curves (load–unload, fibre D).

2.2.4. Discussion

Except fibre G, which was spun from isotropic pitch, M40 and mesophase pitch-based fibres A, B, C and D show this non-linearity: softening in compression and no permanent deformation after removing the load. In Fig. 7, tangent moduli, E_t (normalized by the moduli, E_0, at the zero compressive strain) and their corresponding strains are plotted from the compression test results. While the isotropic pitch-based fibre G does not show the modulus softening, Kevlar 49, M40 and mesophase pitch-based carbon fibres do, and the softening intensifies as the compressive stress increases. Further, as the fibre tensile modulus of mesophase pitch-based fibre increases, the softening starts at a smaller compressive strain and intensifies. When the compressive load was removed from the Kevlar 49 fibre-reinforced coupons, they left permanent deformation, as reported in other works [3, 7, 13], in which the kink band formation in fibres was proposed. On the other hand, M40 and mesophase pitch-based carbon fibre composites showed no permanent deformation after the load removal.

There have been many attempts to investigate compressive deformation and failure mechanisms in unidirectional composites [13–16], taking account of the

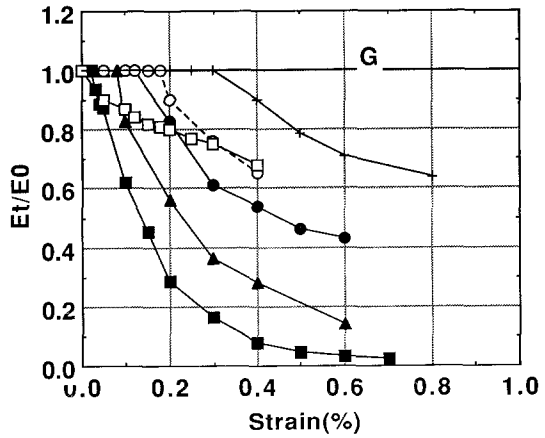

Figure 7 Compressive tangent moduli versus strain. (– + –) A, (–●–) B, (–▲–) C, (–■–) D, (–□–) M40, (––○––) Kevlar 49, (—) G.

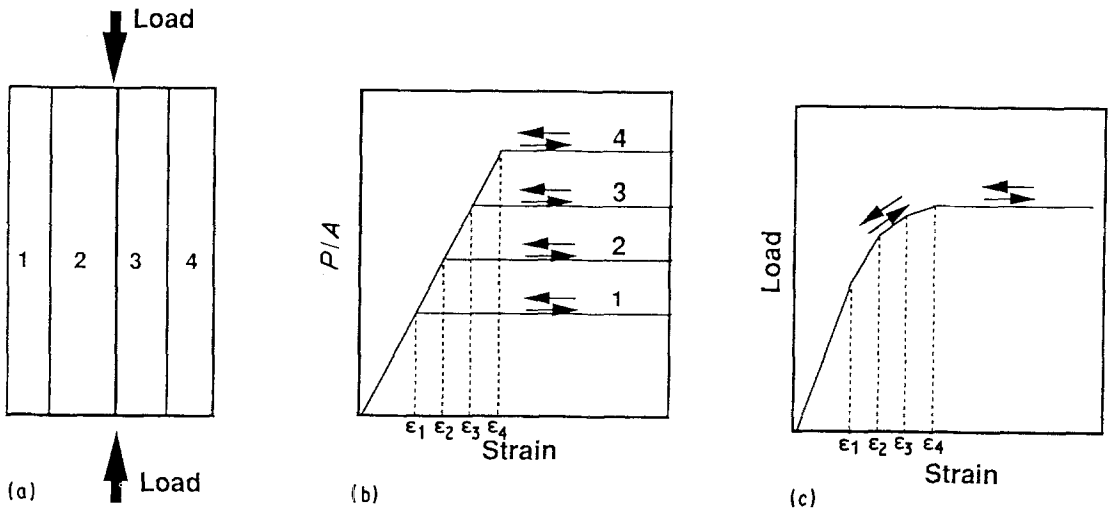

Figure 8 Sublayers model for non-linear compression behaviour. P is compressive load, A is cross-sectional area.

effects of laminate initial imperfections, such as out-of-plane waviness and in-plane waviness of fibres or resin non-linearities. However, these attempts seem to be unable to explain the large non-linear stress–strain relation in the small strain region which we have observed. If a resin material non-linearity is considered to be associated with shear plastic deformation, and if matrix non-linearity plays a significant role, then there must be significant permanent deformation after removing the applied load. If some laminate imperfections play a significant role, they need to be associated with relatively larger strain, say, much larger than 0.5%. From the plots in [15, 16], the laminate imperfections may not be able to predict the large non-linearity.

Because the magnitude of softening is very large and there is no permanent deformation after the compressive load removal, the deformation mechanisms can be thought of as associated with local elastic buckling along the fibre direction. As shown in Fig. 8a, a unidirectional composite consists of several sublayers and each layer behaves as shown in Fig. 8b under compression. Each layer is initially an elastic material of a compressive modulus at zero strain and loses stiffness completely after the compressive strain becomes ε_i for the ith layer, and when unloaded it traces back the loading path. This is modelled by keeping the Euler buckling of a column under compression in mind. Then, the stress–strain relation of the composites becomes the one illustrated in Fig. 8c and the strain is completely removed when the load is removed.

As the fibre modulus increases, the fibre surface becomes more difficult to oxidize during the surface treatment, and, consequently, it is more difficult to get a proper fibre and matrix interface which may prevent the local bucklings. This increase in the difficulty of surface treatment with the increasing fibre modulus might be associated with the increasing intensity of compression non-linearity also with the increasing fibre modulus. The increasing fibre modulus with the increasing anisotropy, i.e. the decreasing fibre torsional modulus, might be associated with local bucklings which could also explain the sublayer behaviour of the unidirectional composite under the longitudinal compression. These two possible mechanisms associated with the compression non-linearity are dealing with fibre and matrix composite characteristics.

On the other hand, graphite crystallites of high modulus mesophase pitch-based fibre are highly oriented and highly grown along the fibre axis during the fibre graphitization, which results in a strong tensile property and a weak lateral property. This highly grown and highly oriented basal plane arrangement might be associated with microscopic buckling in fibres. These are possible explanations of mechanisms which may cause behaviour similar to the sublayer stress–strain relation. However, a full understanding of this non-linearity is not yet reached, and we are actively investigating this to get much better composite compressive properties from the fibres.

3. Three-point bending test analysis

3.1. Test method and analytical model

When composite plates are fabricated from the fibres with those observed non-linear behaviours in compression, if they deform with compressive and tensile strains simultaneously, they behave considerably differently from plates with linear material properties. To understand the bending deformation of these composite plates, the three-point bending of a plate reinforced with fibre having the compressive and tensile stress–strain relation shown in Fig. 9 was analysed. This relation closely resembles that of an epoxy matrix unidirectional composite plate reinforced with the fibre D of 54% fibre volume fraction. The material properties of the plate along the thickness direction are 7 GPa for Young's modulus, 0.34 for Poisson's ratio and 6 GPa for the shear modulus. In the analysis, a plate thickness of 2 mm, width of 25 mm and length of 100 mm were used. The boundary conditions are shown in Fig. 10 along with the finite-element model. Each element is an eight-node isoparametric element with the plane-strain assumption.

3.2. Results and discussion

3.2.1. Load–deflection curve

In Fig. 11, the load deflection plot is shown, in which the experimental result (solid line) was obtained from

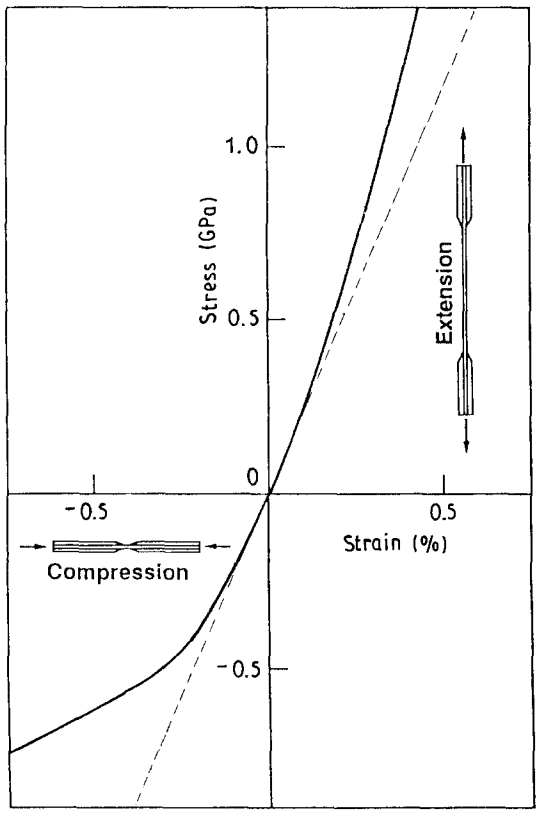

Figure 9 Stress–strain curve of unidirectional composite (fibre D).

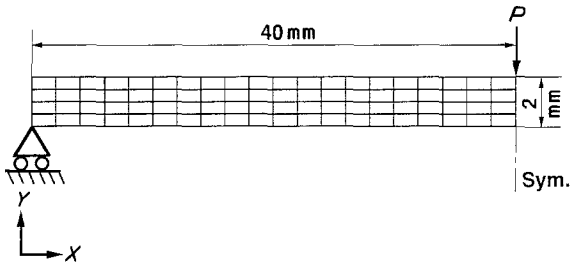

Figure 10 Finite-element model for three-point bending test.

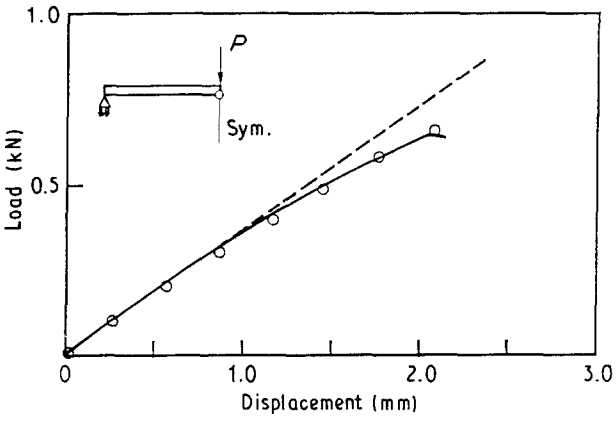

Figure 11 Load–deflection curve. (○) FEM, (——) experiment, (– – –) beam theory.

the fibre D reinforced epoxy unidirectional composite plate of fibre volume fraction 54% and the broken straight line in the same figure was calculated by the linear beam theory with Young's modulus at zero compressive strain. The analysis and experimental results agree well with each other, although the linear analysis deviates from these results. However, the flexural stiffnesses measured at a small deflection and calculated from the linear beam theory coincide.

3.2.2. Load–strain curve

In Fig. 12, compressive and tensile strains on the surface 8 mm away from where the load was applied are plotted from the experiment, and from the non-linear and linear analysis results. All these strains come close to each other. This is because the combination of the rotation of the cross-section about the neutral axis and the neutral axis movement works to make these strains get closer to the linear analysis results.

3.2.3. Load–stress curve

In Fig. 13a and b, the load–stress curves on the surfaces at the applied load point are shown for linear (broken line) and non-linear (solid line) analysis results. Initially, both the linear and non-linear analysis results agree well with each other, and then deviate from each other as the load increases. The non-linear tensile stress becomes larger and the compressive stress becomes smaller due to the non-linear stress–strain relation and the neutral axis movement. In Fig. 14, the stress and strain distributions on the cross-section at 2 mm from the centre are shown along with the applied loads. As the load increases, the neutral axis moves to the tension side (to the lower side in the figure). As we can expect from Timoshenko's beam assumption, the cross-section remains straight and also perpendicular to the neutral axis. However, the stress distribution in the cross-section becomes highly non-linear as the load increases.

3.2.4. Discussion

The non-linear analysis and experimental results coincide well with each other. But the load–deflection curve obtained by the linear analysis shows a small

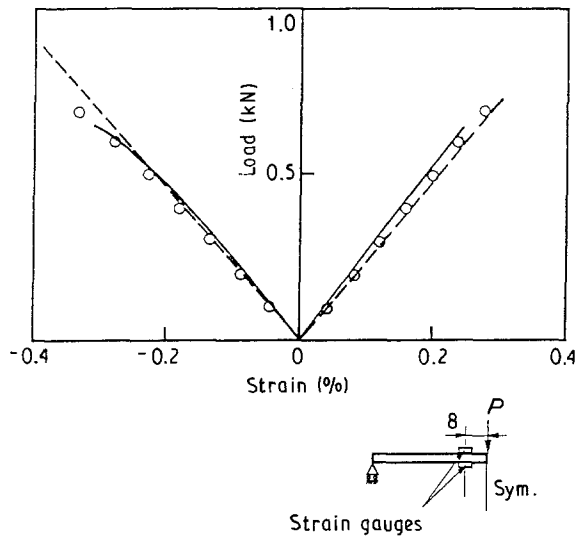

Figure 12 Load–strain curve. (○) FEM, (——) experiment, (– – –) beam theory.

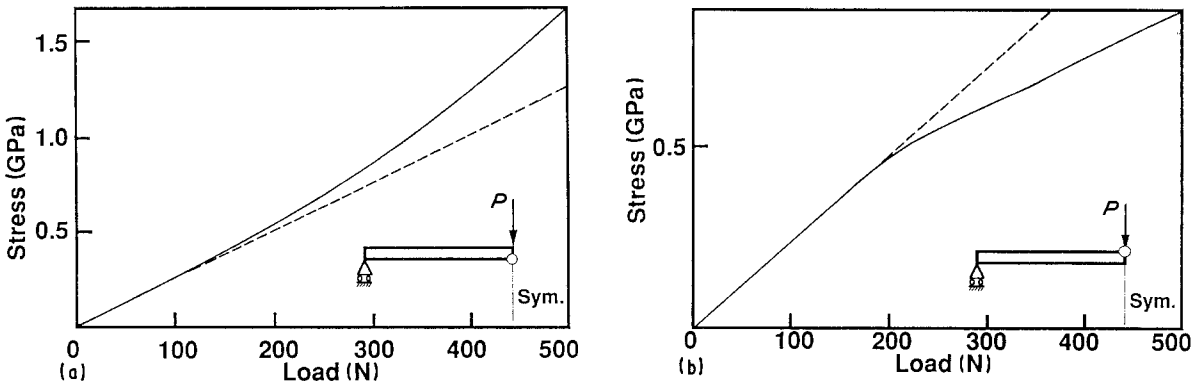

Figure 13 Load–stress curves: (a) tension side, (b) compression side. (——) FEM, (– – –) beam theory.

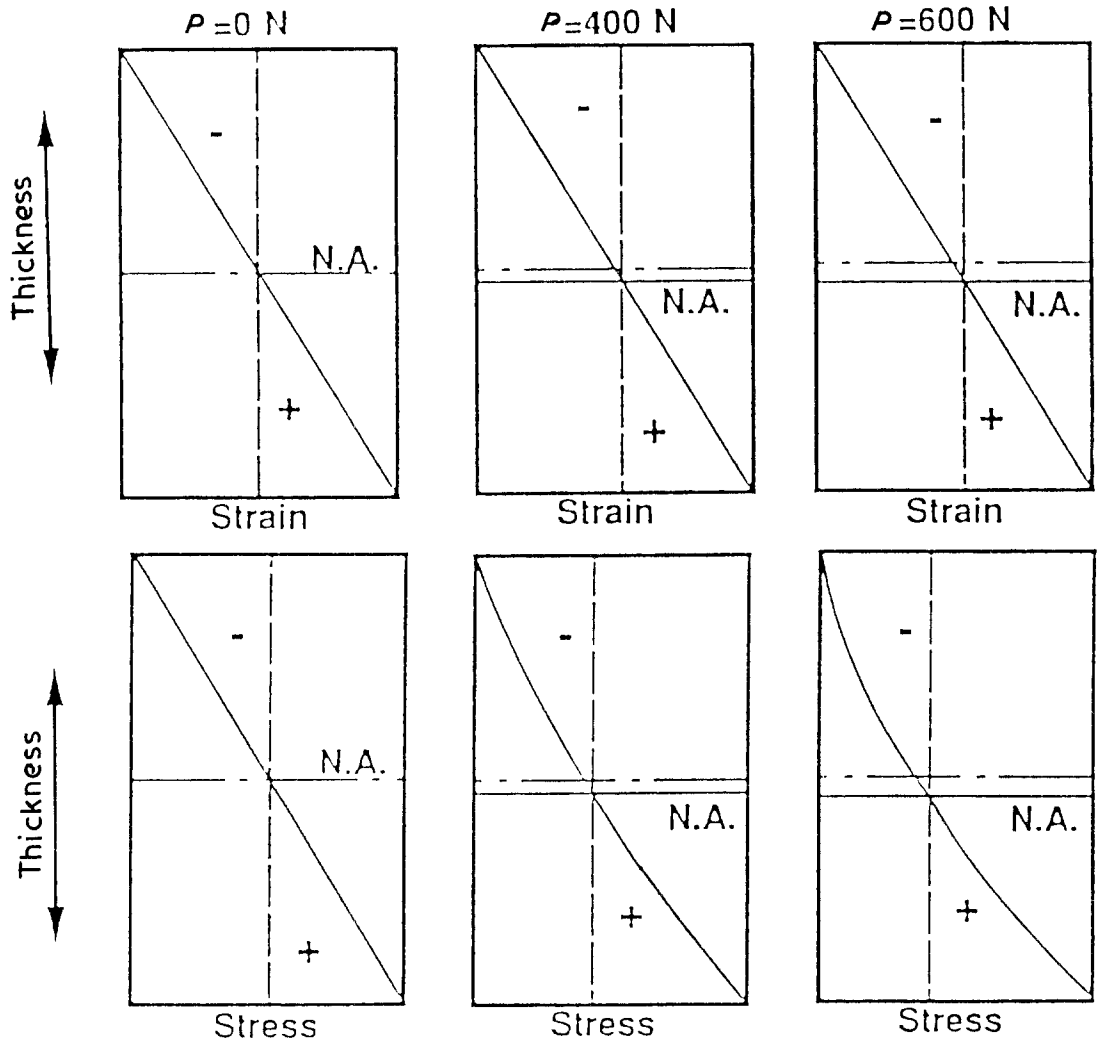

Figure 14 Strain and stress distributions on the cross-section.

deviation from the experimental result for a small load and large deviations at larger strains. Thus the linear analysis is not able to predict the structural behaviour at large deflections. However, the flexural modulus at small strains can be obtained by the linear analysis formula. Because of softening in compression and hardening in tension, the neutral axis shifts to the tension side when the bending moment is applied. As the neutral axis shifts to the tension side and alters the strain distribution across the cross-section, the axis further shifts to the same direction. However, even for a material with such severe non-linearities, the amount of axis shift is about 5% at the failure stress of 700 N. Thus the strains in compression and tension sides are almost the same because of Timoshenko's assumption. On the other hand, differences between compressive and tensile stresses are significantly large due to material non-linearity. For the present material, the maximum tensile stress is about 60% larger than the maximum compressive stress at the failure load. Because the tensile strength of this material is about three times larger than the compressive strength, the coupon failure starts in the compression side, which is consistent with the test result.

4. Conclusion

Unidirectional composites reinforced with mesophase pitch-based high modulus carbon fibres show strong softening under the longitudinal compressive load, and this softening is not associated with permanent deformation. Further, the amount of softening is strongly correlated with fibre tensile modulus: the softening increases with increasing modulus.

The linear beam theory can be applied to the calculation of flexural beam bending stiffness but is not appropriate for calculating the beam failure stress and deformation. Finite-element analysis with severe material non-linearity can predict deflection and stress properly. The stress distribution changes in a highly non-linear manner as the applied load increases.

References

1. W. WATT and B. V. PEROV (eds), "Strong fibers", Handbook of Composites, vol. 1 (Elsevier Science Publishers B.V., The Netherlands, 1985).
2. D. SINCLAIR, *J. Appl. Phys.* **21** (1950) 380.
3. S. J. DETERESA, R. S. PORTER and R. J. FARRIS, *J. Mater. Sci.* **23** (1988) 1886.
4. H. W. HAWTHRONE and E. TEGHTSOONIAN, *J. Mater. Sci.* **10** (1975) 41.
5. S. R. ALLEN, *J. Mater. Sci.* **22** (1987) 853.
6. T. OHSAWA, M. MIWA, M. KAWADA and E. TSUSHIMA, *J. Appl. Polymer Sci.* **39** (1990) 1773.
7. C. ZWEBEN, *J. Composite Mater.* **12** (1973) 422.
8. T. R. GUESS and E. D. REDDY Jr, "An experimental and theoretical study of the bending behavior of Kevlar 49/epoxy beams and rings" in 19th International SAMPE Technical Conference, October, 1987.
9. S. FISCHER and G. MAROM, *Fiber Sci. Technol.* **20** (1984) 91.
10. T. NORITA, A. KITANO and K. NOGUCHI, "Compressive strength of fiber reinforced composite materials – effects of fiber properties" in Proceedings of the 4th Japan–US Conference on Composite Materials, June 1988, Washington, D.C.
11. Standard test method for compressive properties of unidirectional or crossply fiber–resin composites. ASTM Standard D 3410–87 (1987).
12. D. H. WOOLSTENCROFT, A. R. CURTIS and R. I. HARESCEUGH, *Composites* **12** (1981) 275.
13. H. T. HAHN and J. G. WILLIAMS, "Compression failure mechanisms in unidirectional composites", in Testing and Design (Seventh Conference), ASTM STP 893 (1986) pp. 115–139.
14. N. L. HANCOX, *J. Mater. Sci.* **10** (1975) 234.
15. M. J. SHUART, *AIAA J.* **27** (1989) 1274.
16. J. R. YEH and J. L. TEPLY, *J. Composite Mater.* **22** (1988) 245.

Received 18 March
and accepted 1 July 1991